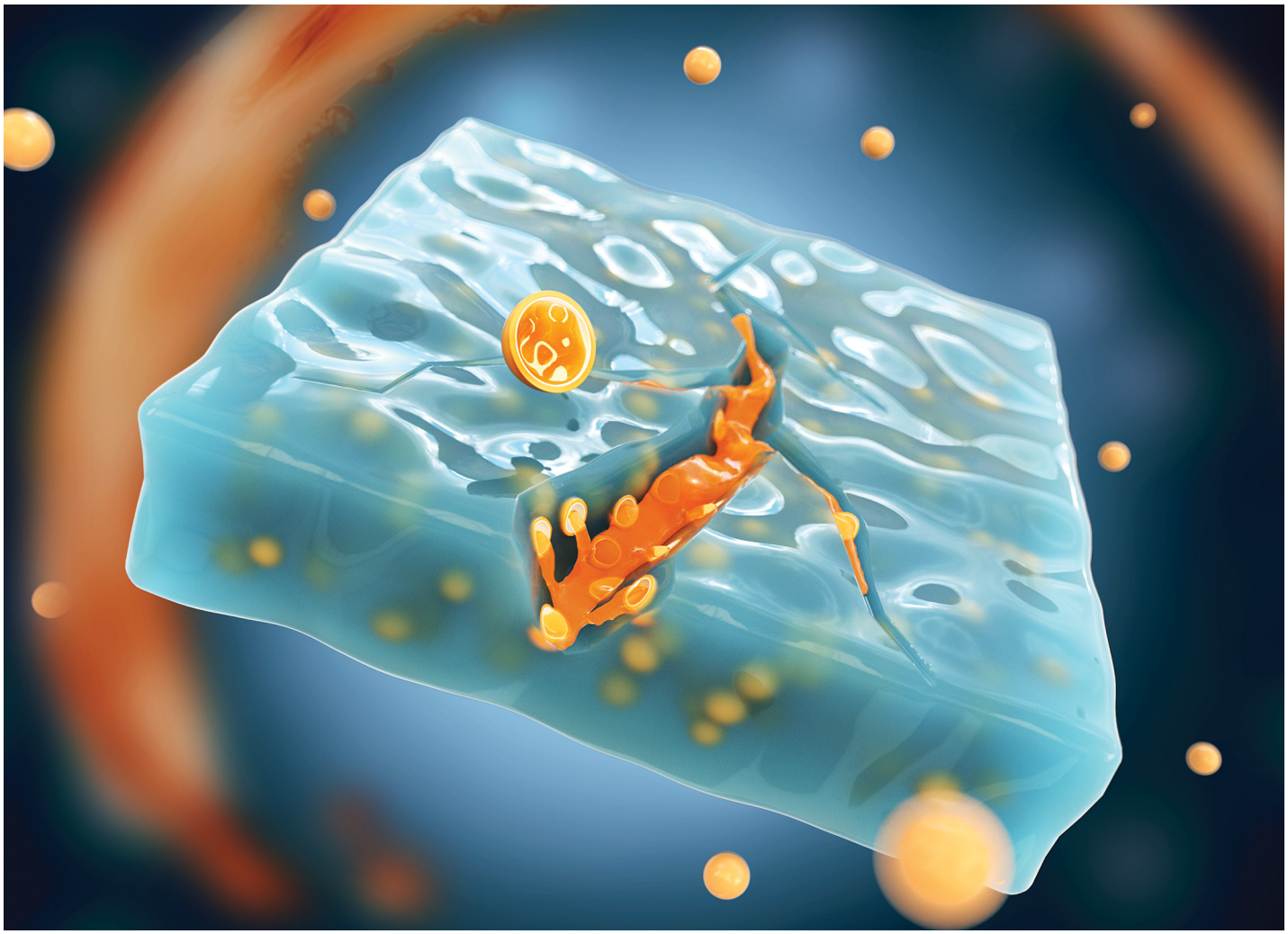

Showcasing research from Professor Yunjun Luo's Functional Polymer Materials Laboratory, School of Materials Science & Engineering, University of Beijing Institute of Technology, Beijing.

Room temperature self-healing epoxy waterborne polyurethane containing microcapsules with waterborne polyurethane shells and mercaptan cores

Based on the theory of Hydrophilic–lipophilic balance value (HLB), we measured the HLB value of Pentaerythritol tetrakis(3-mercaptopropionate) (PETMP) to be 12.6. Utilizing this value, we encapsulated it into microcapsules and embedded these microcapsules in the Epoxy Waterborne Polyurethane (EWPU) matrix. When this EWPU was microcracked, the microcapsules will break and the PETMP will release to the valley of the microcrack to rebond the two faces of the microcrack, achieving the target of self-healing.

As featured in:

See Yunjun Luo *et al.*, *Mater. Adv.*, 2022, **3**, 7015.

ROYAL SOCIETY OF CHEMISTRY

rsc.li/materials-advances

Registered charity number: 207890

Materials Advances

ROYAL SOCIETY OF CHEMISTRY

PAPER

View Article Online
View Journal | View Issue

Cite this: *Mater. Adv.*, 2022, 3, 7015

Room temperature self-healing epoxy waterborne polyurethane containing microcapsules with waterborne polyurethane shells and mercaptan cores

Mengyun Zhang,[ab] Rimin Cong[a] and Yunjun Luo *[a]

Regardless of various strategies for preparing microcapsules to obtain self-healing materials with high efficiencies, it remains a significant challenge to use suitable shell materials to capsulate mercaptans due to their high reactivity. Herein, we report a simple method to utilize waterborne polyurethane (WPU) prepolymers which have priorities to react with diethylenetriamine (DETA) over thiol functional groups to make pentaerythritol tetrakis(3-mercaptopropionate) (PETMP) incorporated into microcapsules successfully. Self-healing epoxy waterborne polyurethane (EWPU) was prepared by embedding this kind of microcapsule into the matrix. Once microcracks expand, microcapsules break and release PETMP to the valley of the microcrack to react with epoxy functional groups under the self-catalytic effects of triethylamine (TEA), making microcracks recover to the original state and reaching the self-healing target. The spherical morphology of microcapsules is affected by the TEA content that is determined to be 60% of the theoretical value for totally neutralizing 2-bis (hydroxymethyl) propionic acid (DMPA) in WPU prepolymers. Microcapsule components have been confirmed by FTIR spectroscopy. The core content of PETMP is about 60.66% resulting from TG analysis. The best self-healing conditions for EWPU include 8 wt% microcapsules and healing at room temperature for 2 days. The net self-healing efficiency could reach nearly 100%. In addition, the hydrophilic–lipophilic balance (HLB) values of emulsions are investigated by the droplet size test method. The HLB value of PETMP has been deduced to be 12.2, offering theoretical guidance to explore the emulsion properties. Finally, this efficient and straightforward preparation technology provides potential application values for self-healing materials in industry.

Received 25th January 2022,
Accepted 3rd August 2022

DOI: 10.1039/d2ma00085g

rsc.li/materials-advances

1 Introduction

Waterborne polyurethane (WPU) with tunable flexibility and toughness provides great application values for coatings and adhesives.[1–4] Its ability to resist compact or damage allows it to be used in special areas such as automobiles, aerospace, and architecture. In some cases, WPU must show good usability and long service life as functional protective materials, especially in some critical technology fields when special needs are considered. However, the structural integrity of WPU would be gradually destroyed by microcracks which are deeply hidden in the matrix and difficult to detect visually due to a long-time exposure to harsh environmental conditions or suffering from the rigorous external stimuli. To solve the microcrack problem, self-healing waterborne polyurethane (SHWPU) has been proposed. For example, SHWPU based on 2-hydroxyethyl disulfide (HEDS) possesses shape memory effects assisting the self-healing properties, and could self-heal at 65 °C.[5] Similarly, shape memory effects could be described as cohesive behaviors which play significant roles in the prophase of the self-healing process.[6] Unfortunately, the self-healing process should be realized with external stimuli such as heat.[7] Although SHWPU could self-heal under suitable conditions, S–S bonds imparted will be weak breaking points compared with C–C bonds, resulting in the decrease of the tensile properties. In addition, the mechanical properties should be improved while maintaining the self-healing properties, which could be achieved through the incorporation of cross-linkers.[8]

To date, disulfide bonds have been the most commonly used self-healing element attributed to dynamic reversible chemistry. Dynamic reversible chemistry contains multiple self-healing elements like Diels–Alder reactions,[9,10] transesterification reactions,[11,12] disulfide exchanges,[13,14] metallophilic

[a] School of Materials Science and Engineering, Beijing Institute of Technology, Beijing 100081, P. R. China. E-mail: yjluo@bit.edu.cn; Tel: +86 01068913689
[b] Institute of Nuclear and New Energy Technology, Tsinghua University, 100084, Beijing, China

attractions,[15,16] hydrogen bonds,[17,18] supramolecular attractions[19,20] and ionic interactions[21]. Nevertheless, only Diels–Alder reactions[22] and disulfide bonds[5] have been successfully introduced into SHWPU. Compared with SHWPU based on dynamic reversible covalent bonds, reports on SHWPU containing microcapsules are scarce.[23] Introducing self-healing microcapsules to the polymer has the advantages of not only enhancing the strength of the matrix with suitable contents but also changing the microstructure of the matrix around the microcracks due to the curing reactions between healing agents and characteristic functional groups. Meanwhile, self-healing materials embedded with microcapsules are the most easily industrialized technical achievements. So much effort has been made to advance this technology.

The earliest self-healing microcapsules microencapsulated with urea–formaldehyde shells were reported by White *et al.*[24] and they were embedded into epoxy coatings. When the microcrack expanded, microcapsules broke and the self-healing monomer dicyclopentadiene (DCPD) was released to the valley of the microcrack by capillary actions, which could polymerize under the effects of the transition metal catalyst (Grubbs' catalyst) at room temperature in several minutes to yield a tough and highly cross-linked polymer network. Due to the self-healing time being short and the curing temperature being relatively low, it is a significant advantage to reach the target of self-healing at room temperature. Meantime, the self-healing efficiency is as high as 75%. Afterward, a series of self-healing microcapsules used in the epoxy system have been synthesized on the theoretical basis of epoxy–hardener reaction pairs such as amine–epoxy[25,26] and thiol–epoxy.[27–29] Due to amine hardeners being more hydrophilic to water, it is difficult to make microcapsules. Compared with DCPD and amine, mercaptan is a kind of highly reactive hardener for epoxy. So the choice of shell materials to microencapsulate mercaptan is a big challenge. Zhang *et al.*[30] used melamine-formaldehyde prepolymers to microencapsulate mercaptan by *in situ* polymerization. As this curing reaction could occur at a low temperature with tertiary amine catalysts, the big challenge is how to reasonably design the structures of self-healing epoxy waterborne polyurethane by introducing reaction pairs between the mercaptan and epoxy groups to achieve the self-healing target at room temperature.

To realize the self-healing performance of WPU, we also consider imparting the epoxy–mercaptan reaction pair to the WPU system. The WPU matrix was modified by epoxy resins to obtain epoxy waterborne polyurethane (EWPU). Then microcapsules with WPU shells and mercaptan cores were prepared and then blended into the EWPU. When the film was scratched, the self-healing agent PETMP released into the microcrack and reacted with the epoxy-functional groups of EWPU to rebond the two faces of the microcrack under the self-catalytic effects of TEA, reaching the target of self-healing. In the present study, we report a simple method to prepare self-healing microcapsules. The morphology of microcapsules was characterized by optical microscopy (OM) and scanning electron microscopy (SEM). The structures of microcapsules, cores, and shells were analyzed by FTIR spectroscopy. The components of microcapsules were tested and computed by thermal gravity (TG) analysis. Then the self-healing efficiency was computed by tensile mechanics and the self-healing process was monitored using an optical microscope combined with a linkam hot stage. Finally, the cross-sectional morphology was also observed by SEM, further verifying the self-healing mechanism.

2 Experimental section

2.1 Materials

Polypropylene glycols (PPG-400, $\overline{M_n} = 400$ g mol^{-1} and PPG-N210, $\overline{M_n} = 1000$ g mol^{-1}) purchased from Tianjin Petrochemical Co., Ltd (China) were dehydrated at 100 °C for 6 h before use. Isophorone diisocyanate (IPDI) was bought from Bayer AG (Germany). 2-Bis (hydroxymethyl) propionic acid (DMPA) purchased from Beijing Linshi Fine Chemical & New Material Co., Ltd (China) was dried at 100 °C for 12 h. Triethylamine (TEA), butanone (MEK), and chlorobenzene (CIB) were bought from Tianjin Fuchen Co. (China). Diethylenetriamine (DETA) and pentaerythritol tetrakis(3-mercaptopropionate) (PETMP) were purchased from Shanghai Saen Chemical Technology Co., Ltd (China). Surfactants Span80 and Tween 80 were bought from Tianjin Guangfu Fine Chemical Research Institute (China). Epoxy resin E-44 was purchased from Fei Cheng De Yuan Chemical Technology Co., Ltd (China). Ultrapure water (18.2 MΩ cm) was used throughout this work.

2.2 Preparation of self-healing microcapsules

Synthesis of waterborne polyurethane prepolymers. Quantified amounts of PPG-400 (10 g, 0.025 mol), DMPA (3 g, 0.022 mol), and IPDI (31.60 g, 0.142 mol) were added into a 250 ml four-necked flask equipped with a mechanical stirrer, a condenser, and nitrogen inlets and allowed to react at 85 °C for 3 h. If the viscosity of reactants increased, the solvent CIB (22.30 g, 0.198 mol) was added at separate times to decrease the viscosity.

Preparation of the oil/water (O/W) emulsion. Water (30 g, 1.667 mol) was poured into a 250 ml beaker. Then the homogeneous mixtures of PETMP (4.5 g, 0.009 mol), CIB (4.5 g, 0.040 mol), and a certain ratio of Span80 and Tween80 were poured into the water phase. Afterward, the emulsion was acquired by emulsifying for 5 min.

Preparation of self-healing microcapsules. The co-solvent of CIB (1.25 g, 0.011 mol) was added into the WPU prepolymers (5.25 g) together with TEA (0.12 g, 0.002 mol) for homogenization. Then, the above mixture was added to the oil/water emulsion quickly at a stirring velocity of 500 rpm followed by adding aqueous DETA (5 g, 0.1 g g^{-1}) immediately. After reacting for 5 min, the self-healing microcapsules were obtained. To make sure that polyaddition reactions between WPU prepolymers and DETA were completed, the microcapsule emulsion rested at room temperature for 30 min. After this, the post-treatments of microcapsules were conducted by washing with water and resting and then repeating several times. Finally, the wet microcapsules were poured into a Petri dish and allowed to dry at room temperature for seven days.

2.3 Preparation of self-healing films

Epoxy waterborne polyurethane (EWPU) was prepared based on the acetone method. 30 g of polypropylene glycol ($\overline{M_n} = 1000$ g mol^{-1}), 20 g of IPDI, and 3 g of DMPA were added into a 250 ml four-necked flask connected with a mechanical stirrer, a nitrogen inlet, and a condenser and allowed to react at 90 °C for 3 h. Then the temperature was decreased to 70 °C; 1.45 g of BDO and 1.78 g of E-44 were also added to the system to maintain the reaction for another 1 h. If the viscosity increased, a certain amount of MEK was added. After the temperature was down to room temperature, 2.26 g of TEA was added to the mixture to neutralize for 30 min. Fowllowing that, DI water was poured into the mixture and 1 g of EDA with 5 ml of DI water was also added quickly to emulsify for 30 min at 2000 rpm. At last, the removal of MEK using a rotary evaporator was performed at 40 °C for 40 min. The synthesis process is shown in Scheme 1. Self-healing waterborne polyurethane was obtained by introducing different contents of microcapsules to 20 g of the EWPU emulsion to blend homogeneously. Then, most water was removed using a rotary evaporator to obtain highly viscous microcapsule emulsions and poured them into the Teflon molds respectively to dry at room temperature for seven days. Finally, semi-transparent films with the little crude surface were obtained for tests and characterization studies.

2.4 Characterization

Emulsion particle sizes. First, 2.5 g of PETMP and 2.5 g of CIB were blended and 1.5 g compounds of Span80 and Tween80 with the varied HLB values were also added to obtain the homogenous oil phase. Then 10 ml of water was further poured into the oil phase slowly and emulsions were gently rotated rather than shaken fiercely to avoid breaking the structures of natural droplets. The following step was to ultrasound the well-prepared emulsions with a high frequency at room temperature. After resting emulsions for 1 h, the droplet size tests were carried out using a laser particle size instrument (Malvern Zetasizer Nano ZS90). As the test results showed multi-peak distributions, the final results acquired were based on picking up the first peak value since it occupied the largest proportions.

Morphology of microcapsules. The morphology of microcapsules was observed using a Leica Optical microscope DM 2500P. Then, the particle size and shell thickness were obtained using the Image-pro 6.0 plus software. The microcapsules from emulsions were coated on the 10 mm × 10 mm glass plate. Then SEM (Hitachi S-4800 field-emission scanning electron microscope, Hitachi Co. Japan) was performed to observe the morphologies of samples sprayed with gold. The EWPU films were quenched by liquid nitrogen and the section morphologies were also observed after specimens were placed at room

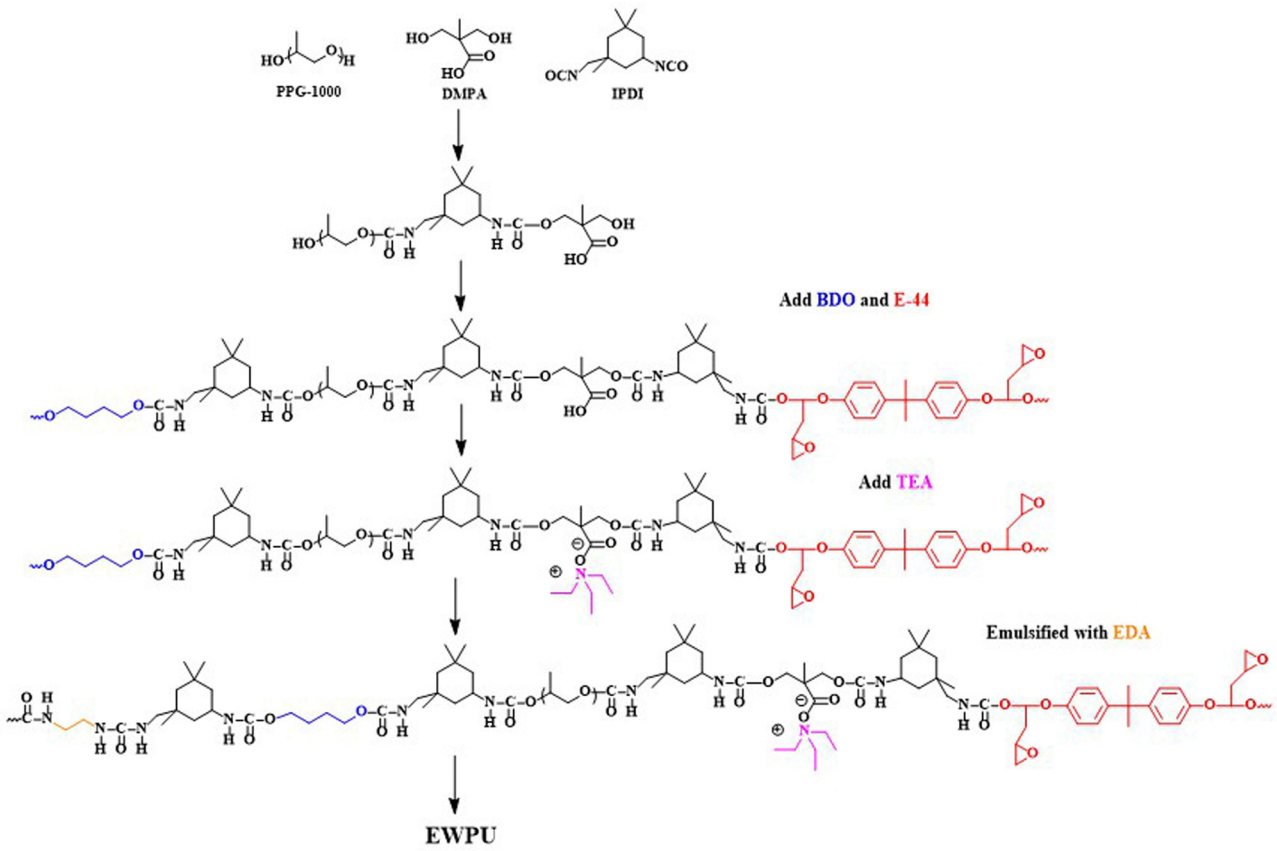

Scheme 1 Synthesis process for EWPU.

temperature for 12 h. In addition, the EWPU films after self-healing for 2 days were pulled off and the section morphologies were also observed.

FTIR characterization. The FTIR instrument used was Nicolet 8700 Fourier transform infrared spectroscopy (FTIR, Thermo Nicolet Corporation). The scan range was from 4000 cm^{-1} to 400 cm^{-1} with a resolution ratio of 4 cm^{-1} in a total time of 48. To characterize the components of microcapsules, partially dried microcapsules were added into the mortar to grind with liquid nitrogen followed by washing with acetone and filtered several times and then dried at room temperature as sample 1. The originally dried microcapsules were used as sample 2. The samples 1 and 2 were mixed with KBr respectively to make tablets for FTIR tests.

Thermogravimetric analysis. The thermal degradation was carried out using Switzerland Mettler TGA/DSC differential thermal scanners. The temperature was increased from 30 °C to 600 °C at a heating rate of 10 °C min^{-1} under the flow of nitrogen; then TG and DTG curves were used to calculate the encapsulation ratio.

Self-healing property evaluations. Monitoring the changes of microcracks on the films of EWPUs was performed using a Leica optical microscope DM 2500P equipped with the Linkam hot stage. Uniaxial tensile tests were carried out using a universal testing machine (Instron-6022, Shimadzu Co., Ltd) at a tensile rate of 100 mm min^{-1} at room temperature. Then, the tensile strength (σ_m) and elongation at break (ε_m) of specimens were measured and the final results were expressed as the average of three samples. Additionally, the microcrack was made using a self-made micrometer scratch instrument with a deepness of about ~0.5 mm on the ~2 mm thickness of films or specimens. The detailed sample preparation information can be found in ref. 6.

3 Results and discussion

3.1 Microcapsule preparation

Self-healing microcapsules have been prepared successfully by the method of *in situ* polymerization combined with emulsion polymerization. Fig. 1 shows the synthesis schematic diagram. Firstly, the mixtures of PETMP, CIB, and surfactants are poured into the water phase and emulsified under a high stirring speed.

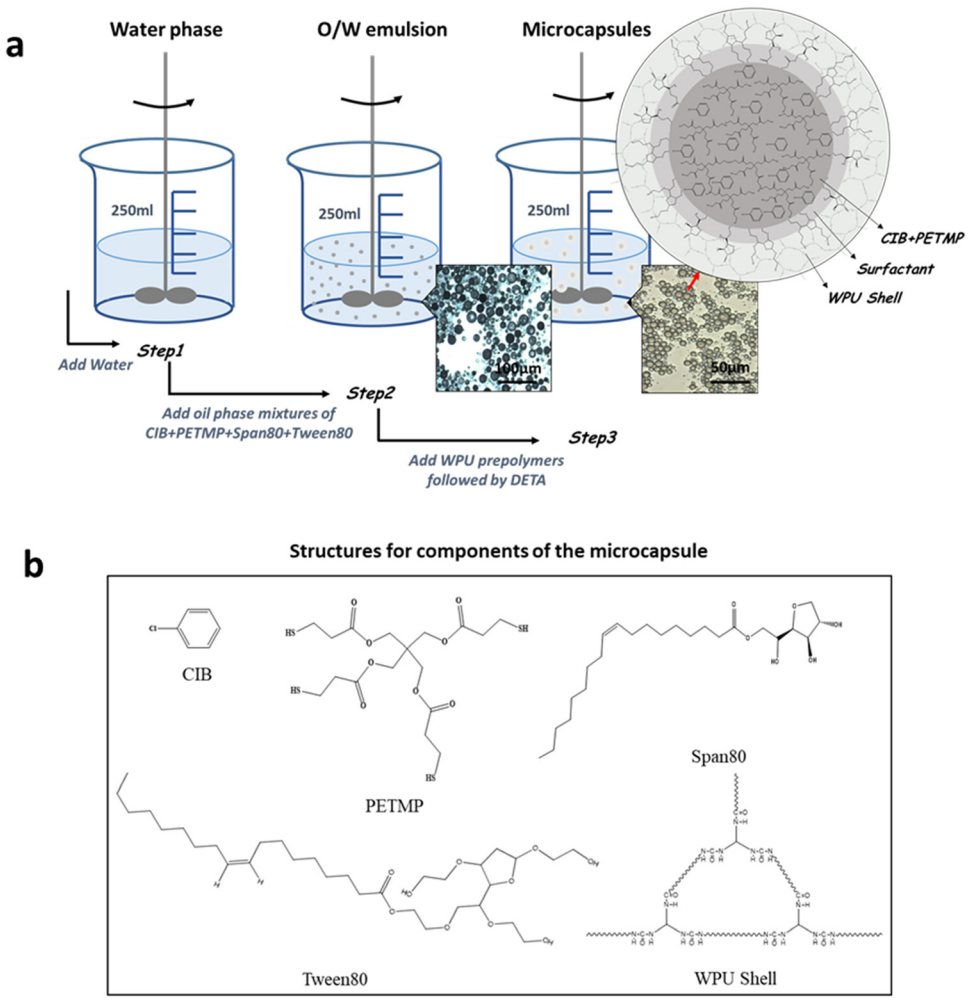

Fig. 1 (a) Preparation process of self-healing microcapsules. (b) Structures for components of the microcapsule.

The mean particle sizes of emulsion droplets are about 20 μm, resulting from the complex interactions of the water phase, oil phase, and the intense shear force. Then WPU prepolymers were added to the emulsion followed by curing with DETA to form shells. The mean particle sizes of microcapsules are about 10 μm, smaller than emulsion droplets, due to the reduced interfacial tension between the oil phase and water phase by WPU prepolymers. The structure of the microcapsule is also shown in Fig. 1. It consists of a WPU shell and a mercaptan core. As the shell should possess a certain strength to resist the external shock, the structure of the WPU shell could be tuned flexibility by changing the styles and content of soft segments and hard segments. Therefore, the smaller molecular weight of polypropylene glycol (PPG) used as soft segments could endow WPU prepolymers with more rigidity. In particular, the linear commercially available PPG-400 is selected to synthesize WPU prepolymers. Furthermore, WPU prepolymers could cure with DETA to form the cross-linking network structure. This structure as the main component of the WPU shell is similar to the EWPU matrix, exhibiting better compatibility and stronger interfacial interactions. DETA chosen here has two advantages. One is that the WPU prepolymers could take precedence over PETMP to react with DETA, shielding the reaction between the WPU prepolymers and PETMP to some degree. The other is that curing reactions take place at room temperature without any external energy input. The core is made up of PETMP and CIB, where CIB can dilute PETMP and decrease the viscosity of PETMP, facilitating the release of PETMP during the self-healing process. Between the core and shell, a layer of surfactants for Span80 and Tween 80 existed, playing the role of the stable dispersion in the preparation of emulsions. This method of preparing microcapsules is simple and easily conducted, which not only saves the cost but also benefits industrialization.

To prepare the external style self-healing EWPU, the microcapsules are blended into the EWPU matrix. When the EWPU matrix produces microcracks, the microcapsules rupture at the same time, releasing the self-healing agent mercaptan into the valley of the microcrack. The mercaptan PETMP is a multifunctional thiol. The self-healing reaction occurs between epoxy groups and thiol groups with the self-catalytic interaction of TEA in the main chains of EWPU. Then the two faces of the microcrack are bonded by curing products, which even enhance the strength of the place around the microcrack, achieving the target of self-healing. In addition, different roles are played by TEA like the neutralization agent, catalytic agent, and morphology modifier.

3.2 Emulsion property explorations

The relationship between HLB values and emulsion properties was explored by tuning the ratio of surfactants for Span80 and Tween80. The droplet size tests were carried out to find the relationship between the particle size and HLB value. The maximal particle size of the emulsion corresponds to the specific HLB value, demonstrating that the emulsifying performance is the best. In other words, the ratio of surfactants for this HLB value can load the most oil phase, which can be regarded as the best suitable surfactants for this oil phase. Meantime, this HLB value is determined to be the exact HLB value of the oil phase. Herein, three series of emulsions were prepared. The first series of emulsions were prepared with HLB values ranging from 6 to 14 at an interval of 1. Then the droplet size tests were conducted to find the optimal HLB range. Based on the first series of emulsion test results, the second series of emulsions were prepared with HLB values ranging from 11.6 to 13.2 at an interval of 0.2 to determine the exact HLB value. Meanwhile, the third series of emulsions were prepared with the pure PETMP oil phase and the HLB values ranging from 11.6 to 13.2 at an interval of 0.2 were used to confirm the HLB value of PETMP.

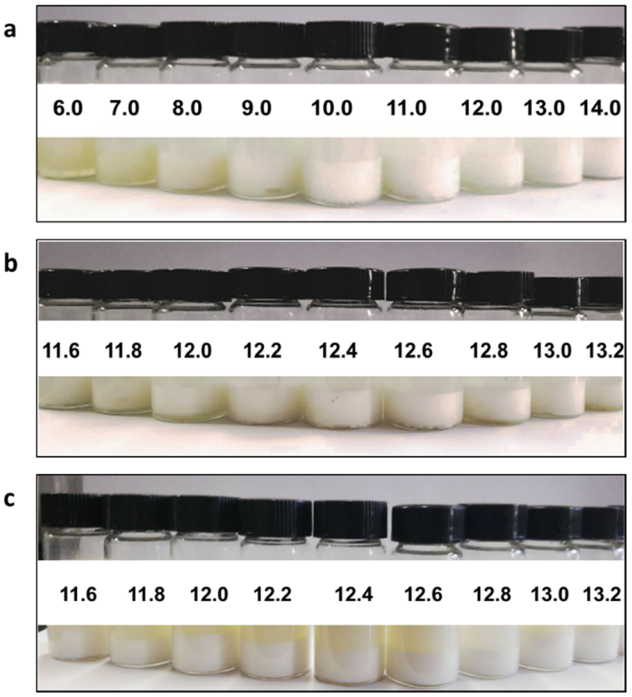

Fig. 2 Photographs of emulsions with different HLB values: (a) the first series, (b) the second series, and (c) the third series.

Fig. 2 shows the photographs of three series of emulsions. As seen in Fig. 2(a), the emulsion colors for the first series are changed from pale yellow to milk-white, indicating that emulsions are transformed from the W/O to O/W states. In Fig. 2(b), the emulsion colors for the second series all exhibit milk-white, which are difficult to judge the emulsion properties. Emulsion particle sizes for three series are listed in Table 1. As seen in data for the first series in Table 1, when the HLB value is less than 10, the particle size exhibits an increasing and decreasing trend, reaching a maximum value of 321.1 nm for the HLB value of 7. Meanwhile, the emulsion is in the W/O state. When the HLB value equals 10, the particle size reaches a minimum value of 177.1 nm, which demonstrates that the emulsion is in a transition state. When the HLB value is larger than 10, the particle size also exhibits the increasing and decreasing trend and reaches a maximum value of 284.2 nm for the HLB value of 13.0, implying that the emulsion is in the O/W state. To obtain

Table 1 Formulations of surfactants Span80 and Tween80 and particle sizes of emulsions

First series				Second series				Third series			
HLB	Span80 (g)	Tween80 (g)	*d* (nm)	*HLB*	Span80 (g)	Tween80 (g)	*d* (nm)	*HLB*	Span80 (g)	Tween80 (g)	*d* (nm)
6	1.26	0.24	280.8	11.6	0.48	1.02	242.5	11.6	0.48	1.02	421.3
7	1.12	0.38	321.1	11.8	0.45	1.05	245.0	11.8	0.45	1.05	483.4
8	0.98	0.52	231.0	12.0	0.42	1.08	251.2	12.0	0.42	1.08	507.5
9	0.84	0.66	191.1	12.2	0.39	1.11	256.6	12.2	0.39	1.11	537.2
10	0.70	0.80	177.1	12.4	0.36	1.14	274.1	12.4	0.36	1.14	455.4
11	0.56	0.94	240.8	12.6	0.34	1.16	404.7	12.6	0.34	1.16	384.3
12	0.42	1.08	251.2	12.8	0.31	1.19	343.7	12.8	0.31	1.19	346.7
13	0.28	1.22	284.2	13.0	0.28	1.22	284.2	13.0	0.28	1.22	307.3
14	0.14	1.36	249.7	13.2	0.25	1.25	261.6	13.2	0.25	1.25	288.9

the optimal and stable emulsion, emulsion droplet sizes for the second series were also tested. While the HLB value is ranged from 11.6 to 13.4, the particle size exhibits the increasing and decreasing trend and reaches a maximum value of 404.7 nm for the HLB value of 12.6. The suitable HLB value of surfactants would obtain the biggest emulsion particle size, benefiting from obtaining the emulsion with the best distribution state of surfactants. So the optimal HLB value for this emulsion is 12.6.

In addition, combining experimental and related theories,[31,32] the HLB value for PETMP can be deduced from eqn (1):

$$HLB_{\text{mix}} = \frac{HLB_{\text{PETMP}} * m_1 + HLB_{\text{CIB}} * m_2}{m_1 + m_2} \quad (1)$$

Here, HLB_{PETMP}, HLB_{CIB}, and HLB_{mix} represent the HLB values of PETMP, CIB, and the emulsion, respectively, where HLB_{CIB} is 13 and HLB_{mix} is 12.6. Besides, m_1 and m_2 are the weights of PETMP and CIB. So the final HLB value of PETMP could be inferred to be 12.2.

Apart from the experimental method, the group contribution addition method could be further used to compute HLB values for different substances. Based on HLB values for all kinds of functional groups[33] together with eqn (2), the HLB value for the group –SH could be deduced to be 0.325, which is much lower than that of 1.9 for the –OH group, indicating that –SH is not very hydrophilic.

$$HLB = 7 + \sum_{i}^{m} H_{\text{Hydrophilic groups}} + \sum_{j}^{n} H_{\text{Lipophilic groups}} \quad (2)$$

where $H_{\text{Hydrophilicgroups}}$ is the HLB value for the hydrophilic group and $H_{\text{Lipophilicgroups}}$ is the HLB value for the lipophilic group, while i and j represent styles of groups and m and n represent numbers of groups, respectively. To confirm the correctness of the HLB value for PETMP, the third series of emulsions were also tested. The particle sizes of the third series of emulsions exhibit the increasing and decreasing trend and reach a maximal value of 537.2 nm for the HLB value of 12.2, which is following the calculated value above, demonstrating that the HLB value of PETMP is credible.

3.3 Morphology analysis

The morphologies of self-healing microcapsules are shown in Fig. 3. Fig. 3(a) shows the optical microscope image, showing that self-healing microcapsules are spherical and particle sizes are uneven. Moreover, some microcapsules are pleated, because larger particles are crushed with the stronger shear force. Fig. 3(b–d) shows SEM images, showing that the particle sizes of microcapsules are about 10 μm with smooth surfaces. Meanwhile, there are many factors to affect the morphology of microcapsules such as the stirring rate, emulsifiers, the O/W ratio, microencapsulation material structures, *etc*, where TEA is an important component of the microencapsulation material and it plays a significant role in the morphology control. For microcapsule shell materials, many carboxyls exist in the main chains of WPU prepolymers, which are neutralized by TEA to form ionic pairs. As the main chains of WPU prepolymers are hydrophobic and ionic pairs are hydrophilic, ionic pairs are randomly distributed on prepolymers, endowing main chains with the hydrophilic properties. Once WPU prepolymers are added to the O/W emulsion, they would quickly distribute around oil droplets at the interfaces of oil and water phases, forming shells with different surface tensions. Additionally, the surface tension is dominantly tuned by the TEA content, making microcapsules exhibit different particle sizes and shell thicknesses. The influence of the TEA content is explored and the experimental results are listed in Fig. 4. As seen in Fig. 4(a), when TEA is absent in WPU prepolymers, these prepolymers incline to coat outside of oil droplets due to their high

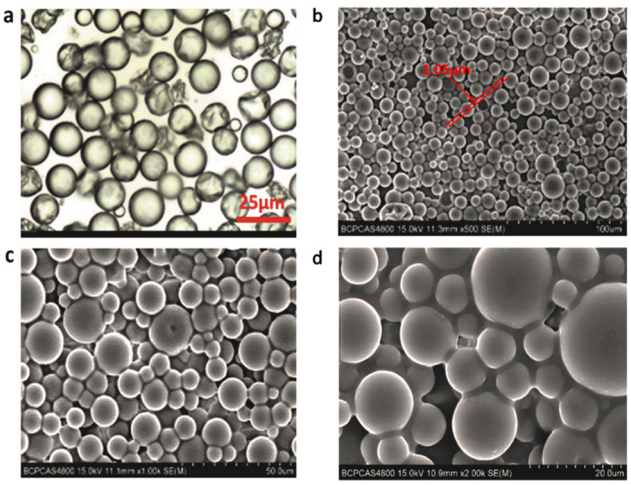

Fig. 3 (a) Optical microscopy and (b–d) SEM images of microcapsules.

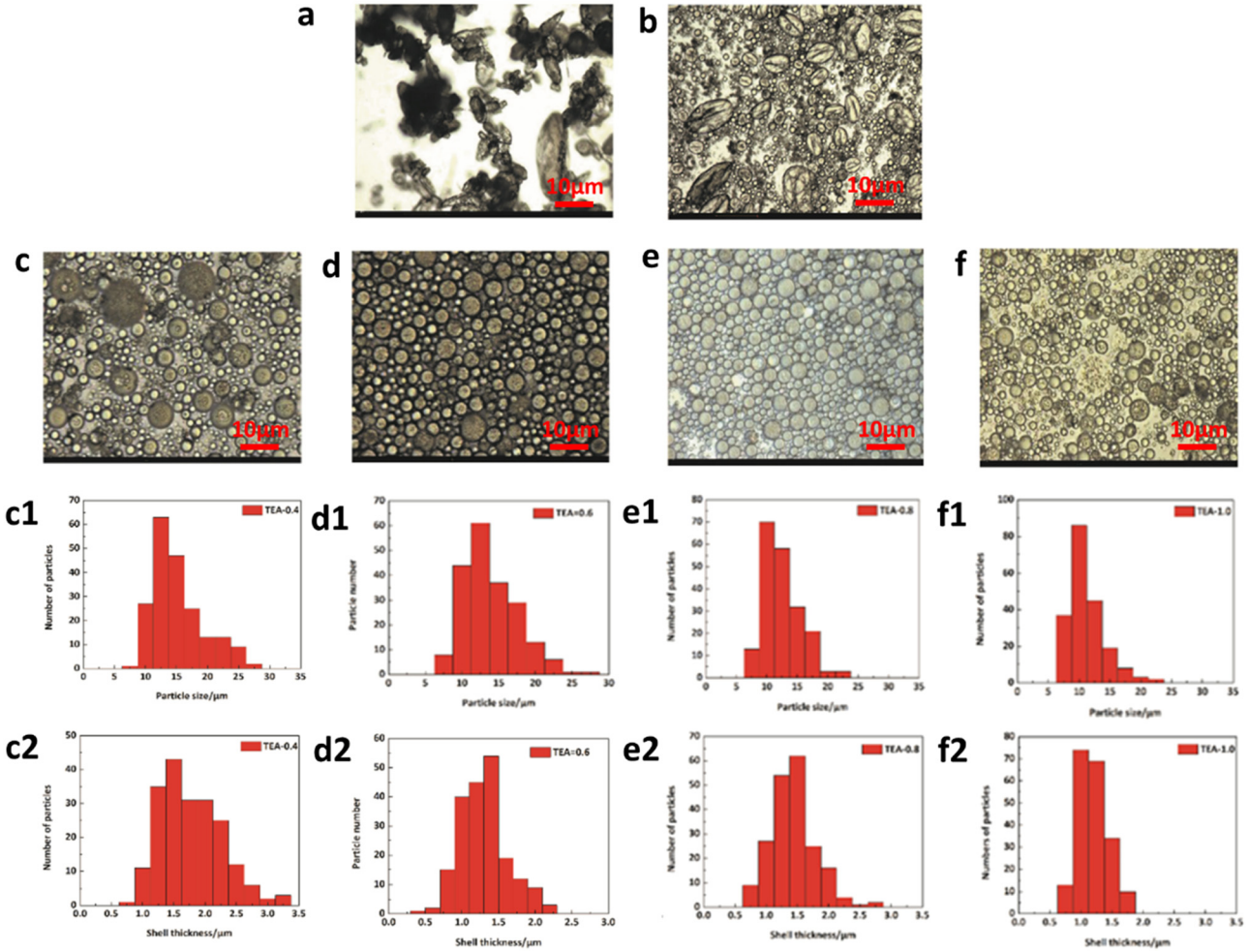

Fig. 4 Optical microscopy images of (a) TEA-0%, (b) TEA-20%, (c) TEA-40%, (d) TEA-60%, (e) TEA-80% and (f) TEA-100%. (c1–f1) Particle size distributions for c–f. (c2–f2) Shell thickness distributions for c–f.

hydrophobic degrees, forming extremely irregular morphologies under the effects of the intense shear force. When the TEA content is less than 60% of the theoretical value (TEA content for completely neutralizing carboxyls in theory), the morphologies of microcapsules shown in Fig. 4(b–c) are spherical and irregular ones co-existed, resulting from the relatively little TEA content. When the TEA content is larger than 60% as shown in Fig. 4(d–f), morphologies are all spherical and particle sizes decrease gradually with the increase of the TEA content. The particle size distribution and shell thickness distribution of microcapsules are shown in Fig. 4(c1–f1) and Fig. 4(c2–f2), which statistics are listed in Table 2. The mean particle sizes for c–f exhibit the decreasing trend and the mean shell thicknesses. The larger steric hindrance of TEA endows microcapsules with a certain buoyant force. Increasing the TEA content results in decreasing the interfacial tension even to microcapsule sizes, prolonging the settling time of microcapsules. When the buoyant force is less than the gravity of the microcapsule, microcapsules are easy to sink and separate. Finally, the TEA content is determined to be 60% of the theoretical value, assuring better microcapsule morphology and a quick separation velocity. Meantime, the mean particle size is 12.58 μm and the mean shell thickness is 1.54 μm.

Table 2 Particle size and shell thickness of the microcapsules with different TEA contents

TEA	40 (%)	60 (%)	80 (%)	100 (%)
Particle size (μm)	14.04	12.58	11.21	9.93
Shell thickness (μm)	1.66	1.54	1.32	1.09

3.4 Chemical structure of microcapsules

Self-healing microcapsules are constituted of WPU shells and mercaptan cores. The structures of microcapsules, WPU shells, and mercaptan cores are characterized by FTIR spectroscopy. In Fig. 5(a), the peak at 3342 cm^{-1} is ascribed to –NH–. The peak at 3557 cm^{-1} is ascribed to -OH. The peak at 2929 cm^{-1} is ascribed to $-CH_2-$ and $-CH_3$. Additionally, the peak range of 1600–1800 cm^{-1} is ascribed to > C═O in urethane and urea. Meanwhile, these peaks are all appeared in Fig. 5(b) of microcapsule shells, which are attributed to the general characteristic

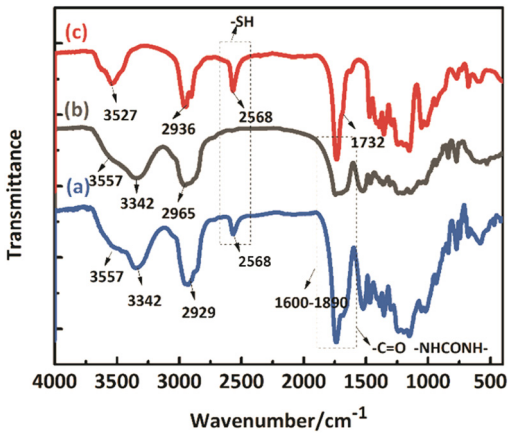

Fig. 5 FTIR spectra of (a) self-healing microcapsules, (b) WPU shells, and (c) PETMP.

absorption peaks of WPU, demonstrating that self-healing microcapsules are indeed encapsulated by WPU. However, the most significant difference between Fig. 5(a and b) is that the peak of 2568 cm^{-1} appeared in Fig. 5(a), which is ascribed to −SH. It is also shown in Fig. 5(c) for the core substance of the mercaptan PETMP, indicating that PETMP is surely contained in microcapsules. It is notable to conclude that the core substance of the mercaptan PETMP is successfully encapsulated by WPU shells.

3.5 Thermal properties and component analysis

To determine the content of microcapsule components, TG tests were carried out. Fig. 6(a and b) shows the TG and DTG curves of the microcapsules, shells, and cores of PETMP. The 5% decomposition temperatures of microcapsules, shells, and PETMP are 259.51 °C, 245.99 °C, and 322.02 °C, respectively. Due to the existence of PETMP, the decomposition temperature of microcapsules is delayed, indicating that PETMP could make microcapsules more stable. The 50% decomposition temperatures of microcapsules, shells, and PETMP are 358.80 °C, 326.70 °C, and 387.52 °C, respectively. The 50% decomposition can be regarded as the fastest decomposition stage. Similarly, PETMP also makes this decomposition stage delayed. In Fig. 6(b), the DTG curves of microcapsules, shells, and PETMP are shown. In particular, the DTG curves of microcapsules can be fitted by the DTG curves of shells and PETMP, which need the use of the scaling factors c and d to aid the fitting. Furthermore, a series of relationships can be deduced below:

$$c \times A_{\mathrm{PETMP}} + d \times A_{\mathrm{shell}} = A_{\mathrm{microcapsule}} \tag{3}$$

$$\frac{c}{m^0_{\mathrm{PETMP}}} \times A'_{\mathrm{PETMP}} + \frac{d}{m^0_{\mathrm{Shell}}} \times A'_{\mathrm{Shell}} = \frac{1}{m^0_{\mathrm{microcapsule}}} \times A'_{\mathrm{microcapsule}} \tag{4}$$

$$\frac{c}{m^0_{\mathrm{PETMP}}} \times \frac{dm_{\mathrm{PETMP}}}{dT} + \frac{d}{m^0_{\mathrm{Shell}}} \times \frac{dm_{\mathrm{Shell}}}{dT} = \frac{1}{m^0_{\mathrm{microcapsule}}} \frac{dm}{dT} \tag{5}$$

$$c \times \frac{m_{\mathrm{PETMP}}}{m^0_{\mathrm{PETMP}}} + d \times \frac{m_{\mathrm{Shell}}}{m^0_{\mathrm{Shell}}} = \frac{m_{\mathrm{microcapsule}}}{m^0_{\mathrm{microcapsule}}} \tag{6}$$

The physical meaning of a and b are the weight loss ratios of shells and PETMP to constitute microcapsules in the TG process, respectively. So parameters a, b, c, and d should satisfy the eqn set (7):

$$\begin{cases} a \times m_{\mathrm{PETMP}} + b \times m_{\mathrm{Shell}} = m_{\mathrm{microcapsule}} \\ c \times \dfrac{m_{\mathrm{PETMP}}}{m^0_{\mathrm{PETMP}}} + d \times \dfrac{m_{\mathrm{Shell}}}{m^0_{\mathrm{Shell}}} = \dfrac{m_{\mathrm{microcapsule}}}{m^0_{\mathrm{microcapsule}}} \end{cases} \tag{7}$$

where m_{PETMP}, m_{Shell}, and $m_{\mathrm{microcapsule}}$ are the weight losses of PETMP, shells, and microcapsules, respectively. m^0_{PETMP}, m^0_{Shell}, and $m^0_{\mathrm{microcapsule}}$ are the original weights of PETMP, shells, and microcapsules, respectively. Then the computed results of a and b are 0.2437 and 0.7424,

$$a = c \times \frac{m^0_{\mathrm{microcapsule}}}{m^0_{\mathrm{PETMP}}} = 0.2437, \quad b = d \times \frac{m^0_{\mathrm{microcapsule}}}{m^0_{\mathrm{Shell}}} = 0.7424$$

So

$$m_{\mathrm{PETMP}}\% = c = 60.66\%$$

$$m_{\mathrm{Shell}}\% = d = 39.34\%$$

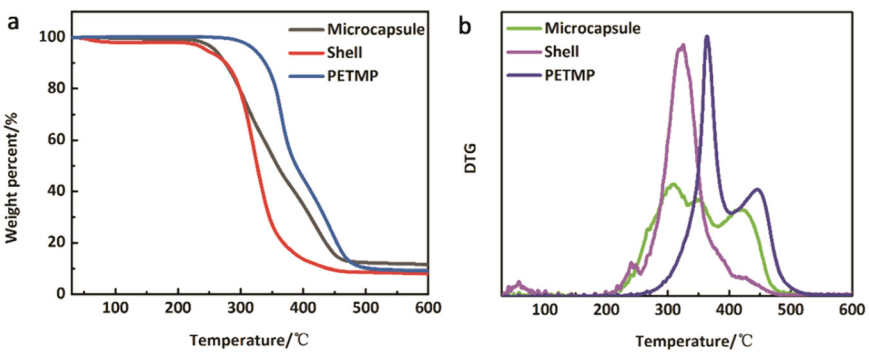

Fig. 6 (a) TG and (b) DTG curves of microcapsules, shells, and PETMP.

Table 3 Decomposition parameters for microcapsules, shells, and PETMP

	$T_{5\%}$[a] (°C)	$T_{50\%}$[b] (°C)	M_{orin} (g)	M_{loss} (g)	$M_{residue}$ (%)
PETMP	322.02	387.52	13.92	13.29	4.53
Shells	245.99	326.70	2.88	2.83	1.74
Microcapsules	259.51	358.80	5.55	5.34	3.78

[a] $T_{5\%}$ and $T_{50\%}$ are the decomposition temperatures of the weight loss with 5% and 50% of PETMP, shells, and microcapsules, respectively. [b] $T_{5\%}$ and $T_{50\%}$ are the decomposition temperatures of the weight loss with 5% and 50% of PETMP, shells, and microcapsules, respectively.

All the relative thermal property parameters are listed in Table 3. On the computed results, the core of PETMP makes up 60.66% of the whole microcapsules.

3.6 Self-healing performance

In theory, mercaptan is a good candidate for curing epoxy functional groups, occurring at room temperature or low temperature. Utilizing this theory, the room temperature self-healing EWPU is designed. To verify its room-temperature self-healing ability, experiments for monitoring changing trends of microcracks at room temperature were carried out. Specifically, pure EWPU and EWPU containing 20 wt% microcapsules with microcracks on them were placed at room temperature, and monitored the changes of microcracks using an optical microscope, which are shown in Fig. 7. The curves of microcrack widths varied with self-healing times for 0 wt%-EWPU and 20 wt%-EWPU are plotted in Fig. 8(a). The self-healing efficiency (SHE) can be calculated based on the eqn (8) which is listed below:

$$\mathrm{SHE} = \left(1 - \frac{d_t}{d_0}\right) \times 100\% \quad (8)$$

where d_t represents the microcrack width at the time of t, and d_0 represents the origin microcrack width at the time of t_0. Then the curves of SHE varied with self-healing times for 0 wt%-EWPU and 20 wt%-EWPU are further plotted in Fig. 8(b).

As can be seen in Fig. 7(a), the microcrack on the pure EWPU is not changing obviously, in which width varies from 10.63 μm to 8.12 μm and the SHE is 23.66% from Fig. 8(a and b), indicating that it possesses a weak self-healing ability. Compared with Fig. 7(a), the microcrack on EWPU containing 20 wt% microcapsules in Fig. 7(b) is changing obviously, in which width varies from 23.5 μm to 10.46 μm and the SHE is 55.42% from Fig. 8(a and b), demonstrating that microcapsules endow EWPU with a certain room temperature self-healing ability. Using the microcrack width to define the SHE can reflect the self-healing behavior to a certain extent, while a more accurate definition can refer to self-healing mechanics.

3.7 Self-healing mechanics

To obtain the external style of self-healing waterborne polyurethane, the different contents of microcapsules (0 wt%–20 wt%) are blended into the EWPU. Resorting to tensile mechanics at room temperature, the net self-healing efficiency can be acquired based on Eqn (9–10) which are listed below:

$$\Delta\mathrm{SHE}_\sigma = \left(\frac{\sigma - \sigma_{0\mathrm{d}-0\mathrm{wt}\%}}{\sigma_{0\mathrm{d}-0\mathrm{wt}\%}} - \frac{\sigma_{0\mathrm{d}} - \sigma_{0\mathrm{d}-0\mathrm{wt}\%}}{\sigma_{0\mathrm{d}-0\mathrm{wt}\%}}\right) \times 100\% \quad (9)$$

$$\Delta\mathrm{SHE}_\varepsilon = \left(\frac{\varepsilon - \varepsilon_{0\mathrm{d}-0\mathrm{wt}\%}}{\varepsilon_{0\mathrm{d}-0\mathrm{wt}\%}} - \frac{\varepsilon_{0\mathrm{d}} - \varepsilon_{0\mathrm{d}-0\mathrm{wt}\%}}{\varepsilon_{0\mathrm{d}-0\mathrm{wt}\%}}\right) \times 100\% \quad (10)$$

where σ is the tensile strength and ε is the elongation at break. Furthermore, the first item in brackets represents the increased strength of the overall mechanical properties of EWPU. The second item in brackets is the influence of microcapsules as fillers on the EWPU matrix. ΔSHE represents the net self-healing efficiency based on molecular diffusions and self-healing ability.

Tables 4 and 5 present the statistics of the tensile strength and elongation at break and Fig. 8 and 9 present the changing trends of ΔSHE for the tensile strength and elongation at break. As can be seen in Table 4, the tensile strength exhibits an increasing and decreasing trend with the increase of the microcapsule content. On the one hand, the microcapsules act as fillers to enhance the tensile strength. On the other hand, the microcapsules rupture, and the self-healing agent PETMP releases into the valley of the microcrack to react with the epoxy-functional groups of the matrix to bond the two faces of the microcrack, which increases the tensile strength of the matrix further. Meanwhile, molecular diffusions also play a significant role in self-healing. In particular, the ΔSHE of the tensile strength for the different contents of microcapsule EWPU samples reaches the maximum value at 8 wt% as shown in Fig. 9(a). Moreover, the tensile strength also exhibits the increasing and then decreasing trend over time. Fig. 9(b) shows that the ΔSHE of the tensile strength reaches the maximum value on the 2nd day. When the time is less than 2 days, the

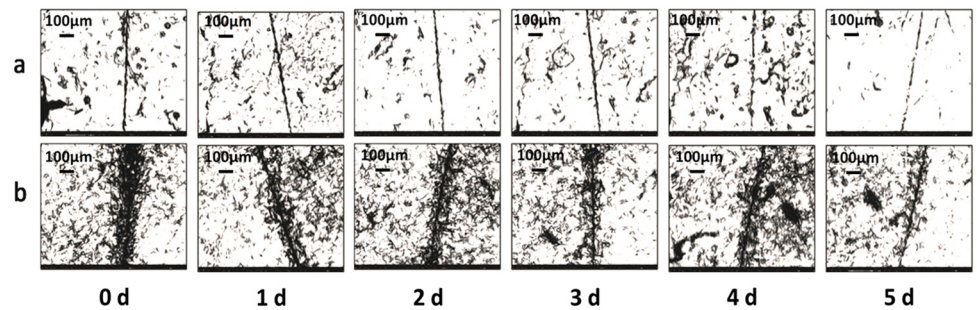

Fig. 7 Self-healing properties of (a) pure EWPU and (b) EWPU with 20% self-healing microcapsules at room temperature for 5 days.

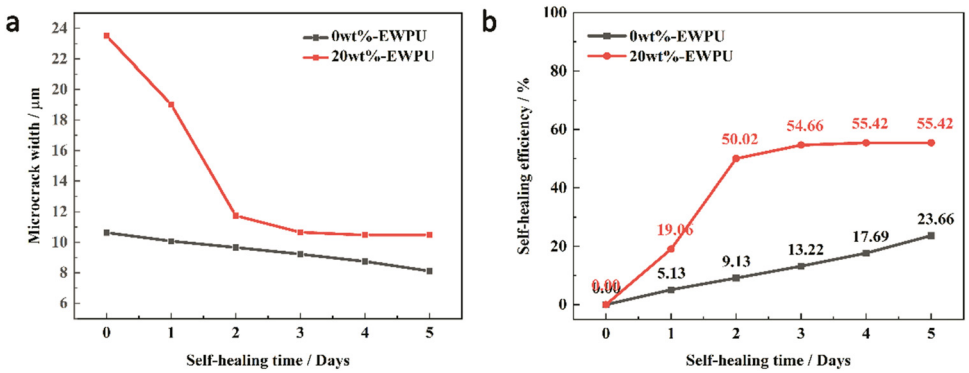

Fig. 8 (a) Microcrack width and (b) self-healing efficiency of samples for 0 wt%-EWPU and 20 wt%-EWPU varied with self-healing times.

Table 4 Mechanical statistics for the tensile strength (Mpa)

	0 d	1 d	2 d	3 d	4 d	5 d
0 wt%	9.22	13.49	15.25	15.36	15.39	15.78
4 wt%	10.36	15.10	17.18	18.52	18.41	17.84
8 wt%	14.78	20.50	24.18	23.84	23.27	21.38
12 wt%	12.35	16.57	19.41	19.02	19.52	18.28
16 wt%	10.57	12.82	13.85	15.60	14.79	14.59
20 wt%	9.64	11.74	11.88	12.58	10.10	9.84

Note: the tensile strength of the sample 0 wt%-EWPU without the microcrack is 17.33 Mpa.

Table 5 Mechanical statistics for the elongation at break (%)

	0 d	1 d	2 d	3 d	4 d	5 d
0 wt%	510.04	597.15	668.67	624.35	614.26	638.51
4 wt%	675.78	870.68	1113.02	991.63	884.72	724.90
8 wt%	765.23	985.24	1256.13	1003.93	995.60	836.63
12 wt%	688.97	895.39	1046.30	923.52	898.48	710.72
16 wt%	657.66	705.13	825.26	724.12	703.76	699.43
20 wt%	568.63	611.60	625.54	628.90	590.77	580.66

Note: the elongation at the break of the sample 0 wt%-EWPU without the microcrack is 847.84%.

self-healing agent PETMP is cured constantly and finally reaches its maximum curing degree on the 2nd day. When the time is more than 2 days, the self-healing agent PETMP is no more curing and begins to act as the role of plasticizers, which decreases the tensile strength. As can be seen in Table 5, the elongation at break also shows the same regular as the tensile strength. Fig. 10 shows that the ΔSHE of the elongation at break is also reaching maximum values at the 8 wt% microcapsule content and the 2nd day respectively due to the same reasons for the tensile strength, which are not detailed anymore. Finally, the best self-healing condition screened out is at the 8 wt% microcapsule content and healing for 2 days.

3.8 Fracture surface

Fig. 11 shows the morphologies of the quenched fracture surface for EWPU containing the different contents of microcapsules. Fig. 11(a) show the morphology of the fracture surface for EWPU without microcapsules. As seen in this figure, the fracture surface is smooth, indicating that the nature of EWPU is homogeneous. Fig. 11(b–f) shows the morphologies of the fracture surface for EWPU containing 4 wt%, 8 wt%, 12 wt%, 16 wt%, and 20 wt% microcapsules. With the increase of microcapsules, many folds exist at the fracture surface and the surface is rough. Fig. 11(i) shows the morphology of the cut fracture surface for EWPU containing 20 wt% microcapsules, showing that different sizes of microcapsules are randomly embedded into the EWPU matrix. When the EWPU films were quenched in liquid nitrogen, the material matrix got shrinking

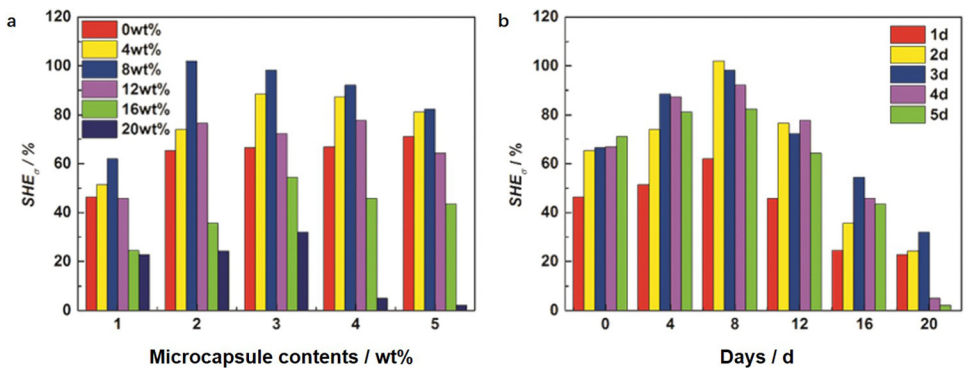

Fig. 9 Self-healing efficiencies for the tensile strength varied with the (a) microcapsule contents and (b) days.

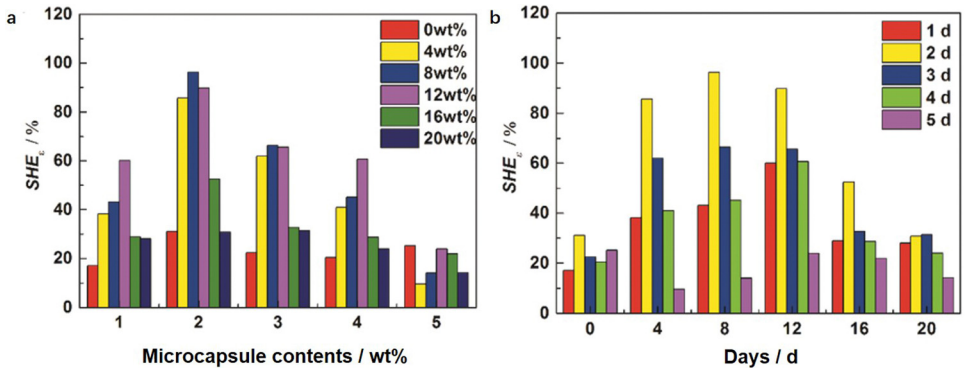

Fig. 10 Self-healing efficiencies for the elongation at break varied with the (a) microcapsule contents and (b) days.

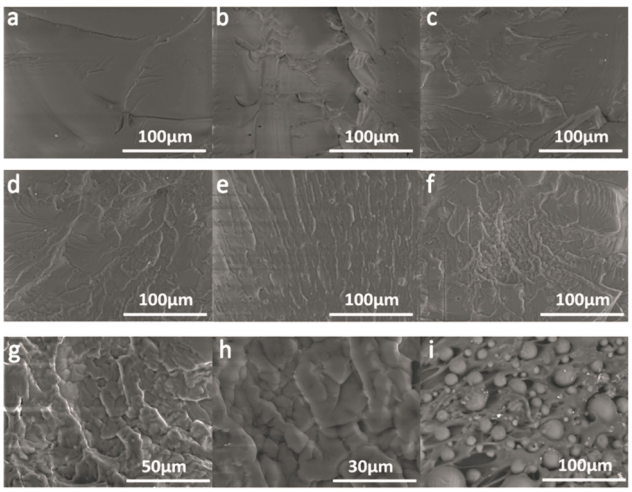

Fig. 11 Morphologies of the quenched fracture surface for EWPU films with the different microcapsule contents: (a) 0 wt%, (b) 4 wt%, (c) 8 wt%, (d) 12 wt%, (e) 16 wt%, (f–h) 20 wt% and except (i) 20 wt% by cut.

and large amounts of the self-healing agent PETMP were released into the microcrack. It is cured with epoxy functional groups under catalytic interactions of TEA in the EWPU main chains, forming a layer of cured products covered on the surface. This layer of cured products makes the fracture surface exhibit many corrugated folds, which bind the fracture surface, demonstrating that self-healing at room temperature could be achieved.

Furthermore, dumbbell specimens with microcracks were carried out with tensile mechanics after healing for 2 days, and the fracture surface was observed using SEM, and the test results are shown in Fig. 12. The morphology of the fracture surface for the specimen without microcapsules is smooth shown in Fig. 12(a). Fig. 12(b) shows that the fracture surface of the specimen with 4 wt% microcapsules possessing little folds and microcapsule particles. Fig. 12(c) shows that the fracture surface of the specimen with 8 wt% microcapsules possessing more folds and microcapsule particles. Combined with the results of tensile mechanics, this sample has better tensile properties and self-healing properties. When the microcapsule content increases to 20 wt%, the morphology of the fracture surface becomes more complex and distributed with more microcapsule particles. These particles function as fillers, which also decrease the tensile strength and impact the self-healing performance.

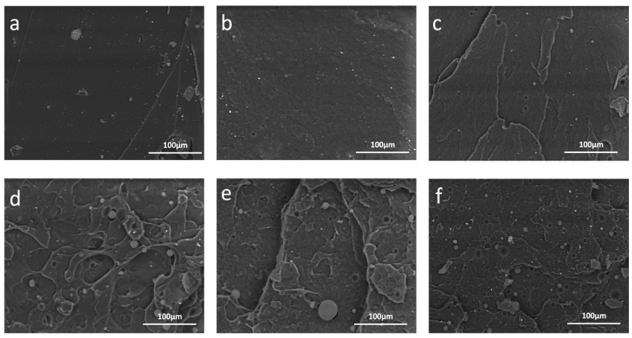

Fig. 12 Morphologies of the tensile fracture surface for EWPU films with the different microcapsule contents: (a) 0 wt%, (b) 4 wt%, (c) 8 wt%, (d) 12 wt%, (e) 16 wt%, and (f) 20 wt%.

4 Conclusions

In summary, we report a simple and efficient method to prepare a kind of self-healing epoxy waterborne polyurethane (EWPU) composite embedded with microcapsules constituted of waterborne polyurethane (WPU) shells and mercaptan cores. Self-healing could be achieved through rupturing the WPU shells of microcapsules, where the mercaptan core PETMP is released to the microcrack and reacted with epoxy-functional groups in the EWPU matrix under the self-catalytic effects of TEA. Apart from this, TEA is imparted by neutralizing the carboxyl of EWPU to make EWPU stably dispersed into the water phase. In addition, TEA plays a significant role in tuning the morphology of microcapsules. FTIR spectra confirm that PETMP cores have been microencapsulated into the microcapsules and the TG analysis results indicate that the core content of PETMP is about 60.66%. Self-healing mechanics and optical microscope observations demonstrate that the best self-healing conditions are the EWPU matrix containing 8% microcapsules and healing at room temperature for 2 days. Apart from this, the

droplet size test is used to measure the HLB values of emulsions and the HLB value of PETMP was also calculated to be 12.2, which is an important parameter for preparing emulsions. This preparation technology is not cumbersome and has a good prospect of industrial applications such as the appearance protection paint of home appliances, automotive, and aviation.

Author contributions

Conceptualization, writing, review, and editing: Mengyun Zhang; methodology, formal analysis, and investigation: Mengyun Zhang and Rimin Cong; resources, visualization, supervision, funding acquisition, and project administration: Yunjun Luo.

Conflicts of interest

All authors have read and agreed to the published version of the manuscript. The authors declare no competing financial interest.

Acknowledgements

The authors are thankful to the National Key Research and Development Program of China (2016YFC0204400).

References

1 I. Bramhecha and J. Sheikh, Development of Sustainable Citric Acid-Based Polyol To Synthesize Waterborne Polyurethane for Antibacterial and Breathable Waterproof Coating of Cotton Fabric, *Ind. Eng. Chem. Res.*, 2019, **58**(47), 21252–21261.
2 V. García-Pacios, V. Costa, M. Colera and J. M. Martín-Martínez, Waterborne polyurethane dispersions obtained with polycarbonate of hexanediol intended for use as coatings, *Prog. Org. Coat.*, 2011, **71**(2), 136–146.
3 A. Lopez, E. Degrandi-Contraires, E. Canetta, C. Creton, J. L. Keddie and J. M. Asua, Waterborne Polyurethane–Acrylic Hybrid Nanoparticles by Miniemulsion Polymerization: Applications in Pressure-Sensitive Adhesives, *Langmuir*, 2011, **27**(7), 3878–3888.
4 I. Díez-García, J. L. Keddie, A. Eceiza and A. Tercjak, Optimization of adhesive performance of waterborne poly (urethane-urea) s for adhesion on high and low surface energy surfaces, *Prog. Org. Coat.*, 2020, **140**, 105495.
5 T. Wan and D. Chen, Synthesis and properties of self-healing waterborne polyurethanes containing disulfide bonds in the main chain, *J. Mater. Sci.*, 2017, **52**(1), 197–207.
6 M. Zhang, F. Zhao and Y. Luo, Self-Healing Mechanism of Microcracks on Waterborne Polyurethane with Tunable Disulfide Bond Contents, *ACS Omega*, 2019, **4**(1), 1703–1714.
7 Y. Xu and D. Chen, A novel self-healing polyurethane based on disulfide bonds, *Macromol. Chem. Phys.*, 2016, **217**(10), 1191–1196.
8 T. Wan and D. Chen, Mechanical enhancement of self-healing waterborne polyurethane by graphene oxide, *Prog. Org. Coat.*, 2018, **121**, 73–79.
9 B. J. Adzima, H. A. Aguirre, C. J. Kloxin, T. F. Scott and C. N. Bowman, Rheological and chemical analysis of reverse gelation in a covalently cross-linked Diels– Alder polymer network, *Macromolecules*, 2008, **41**(23), 9112–9117.
10 C. J. Kloxin and C. N. Bowman, Covalent adaptable networks: smart, reconfigurable and responsive network systems, *Chem. Soc. Rev.*, 2013, **42**(17), 7161–7173.
11 X. Chen, M. A. Dam, K. Ono, A. Mal, H. Shen and S. R. Nutt, *et al.*, A thermally re-mendable cross-linked polymeric material, *Science*, 2002, **295**(5560), 1698–1702.
12 D. Montarnal, M. Capelot, F. Tournilhac and L. Leibler, Silica-like malleable materials from permanent organic networks, *Science*, 2011, **334**(6058), 965–968.
13 A. Rekondo, R. Martin, A. R. de Luzuriaga, G. Cabañero, H. J. Grande and I. Odriozola, Catalyst-free room-temperature self-healing elastomers based on aromatic disulfide metathesis, *Mater. Horiz.*, 2014, **1**(2), 237–240.
14 J. Canadell, H. Goossens and B. Klumperman, Self-Healing Materials Based on Disulfide Links, *Macromolecules*, 2011, **44**(8), 2536–2541.
15 P. Casuso, I. Odriozola, A. Pérez-San Vicente, I. Loinaz, G. Cabañero and H.-J. Grande, *et al.*, Injectable and Self-Healing Dynamic Hydrogels Based on Metal(I)-Thiolate/Disulfide Exchange as Biomaterials with Tunable Mechanical Properties, *Biomacromolecules*, 2015, **16**(11), 3552–3561.
16 S. Bokern, Z. Fan, C. Mattheis, A. Greiner and S. Agarwal, Synthesis of New Thermoplastic Elastomers by Silver Nanoparticles as Cross-Linker, *Macromolecules*, 2011, **44**(12), 5036–5042.
17 P. Cordier, F. Tournilhac, C. Soulié-Ziakovic and L. Leibler, Self-healing and thermoreversible rubber from supramolecular assembly, *Nature*, 2008, **451**(7181), 977–980.
18 Y. Chen and Z. Guan, Multivalent hydrogen bonding block copolymers self-assemble into strong and tough self-healing materials, *Chem. Commun.*, 2014, **50**(74), 10868–10870.
19 S. Burattini, H. M. Colquhoun, B. W. Greenland and W. Hayes, A novel self-healing supramolecular polymer system, *Faraday Discuss.*, 2009, **143**, 251–264.
20 S. Burattini, B. W. Greenland, W. Hayes, M. E. Mackay, S. J. Rowan and H. M. Colquhoun, A supramolecular polymer based on tweezer-type π–π stacking interactions: molecular design for healability and enhanced toughness, *Chem. Mater.*, 2011, **23**(1), 6–8.
21 Q. Wang, J. L. Mynar, M. Yoshida, E. Lee, M. Lee and K. Okuro, *et al.*, High-water-content mouldable hydrogels by mixing clay and a dendritic molecular binder, *Nature*, 2010, **463**(7279), 339–343.
22 Y. Fang, X. Du, Y. Jiang, Z. Du, P. Pan and X. Cheng, *et al.*, Thermal-Driven Self-Healing and Recyclable Waterborne Polyurethane Films Based on Reversible Covalent Interaction, *ACS Sustainable Chem. Eng.*, 2018, **6**(11), 14490–14500.
23 J. Li, Q. Feng, J. Cui, Q. Yuan, H. Qiu and S. Gao, *et al.*, Self-assembled graphene oxide microcapsules in Pickering

emulsions for self-healing waterborne polyurethane coatings, *Compos. Sci. Technol.*, 2017, **151**, 282–290.

24 S. R. White, N. R. Sottos, P. H. Geubelle, J. S. Moore, M. R. Kessler and S. Sriram, *et al.*, Autonomic healing of polymer composites, *Nature*, 2001, **409**(6822), 794–797.

25 D. A. McIlroy, B. J. Blaiszik, M. M. Caruso, S. R. White, J. S. Moore and N. R. Sottos, Microencapsulation of a reactive liquid-phase amine for self-healing epoxy composites, *Macromolecules*, 2010, **43**(4), 1855–1859.

26 H. Yi, Y. Deng and C. Wang, Pickering emulsion-based fabrication of epoxy and amine microcapsules for dual core self-healing coating, *Compos. Sci. Technol.*, 2016, **133**, 51–59.

27 Y. C. Yuan, M. Z. Rong and M. Q. Zhang, Preparation and characterization of microencapsulated polythiol, *Polymer*, 2008, **49**(10), 2531–2541.

28 F. Ahangaran, M. Hayaty, A. H. Navarchian and F. Picchioni, Micromechanical assessment of PMMA microcapsules containing epoxy and mercaptan as self-healing agents, *Polym. Test.*, 2017, **64**, 330–336.

29 E. T. van den Dungen and B. Klumperman, Synthesis of liquid-filled nanocapsules via the miniemulsion technique, *J. Polym. Sci., Part A: Polym. Chem.*, 2010, **48**(22), 5215–5230.

30 Y. C. Yuan, M. Z. Rong, M. Q. Zhang, J. Chen, G. C. Yang and X. M. Li, Self-healing polymeric materials using epoxy/mercaptan as the healant, *Macromolecules*, 2008, **41**(14), 5197–5202.

31 W. C. Griffin, Classification of surface-active agents by ''HLB'', *J. Soc. Cosmet. Chem.*, 1949, **1**, 311–326.

32 W. C. Griffin, Calculation of HLB values of non-ionic surfactants, *J. Soc. Cosmet. Chem.*, 1954, **5**, 249–256.

33 J. R. Kanicky, J.-C. Lopez-Montilla, S. Pandey and D. O. Shah, Surface chemistry in the petroleum industry, *Handb. Appl. Surf. Colloid Chem.*, 2001, **1**, 251–267.